Biophysical Letter

QM/MM Model of the Mouse Olfactory Receptor MOR244-3 Validated by Site-Directed Mutagenesis Experiments

Sivakumar Sekharan,[1,*] Mehmed Z. Ertem,[1,2,*] Hanyi Zhuang,[3,4,*] Eric Block,[5] Hiroaki Matsunami,[6,7] Ruina Zhang,[3] Jennifer N. Wei,[1] Yi Pan,[3] and Victor S. Batista[1,*]

[1]Department of Chemistry, Yale University, New Haven, Connecticut; [2]Chemistry Department, Brookhaven National Laboratory, Upton, New York; [3]Department of Pathophysiology, Key Laboratory of Cell Differentiation and Apoptosis of the Chinese Ministry of Education, Shanghai Jiao Tong University School of Medicine, Shanghai, P. R. China; [4]Institute of Health Sciences, Shanghai Jiao Tong University School of Medicine/Shanghai Institutes for Biological Sciences of Chinese Academy of Sciences, Shanghai, P. R. China; [5]Department of Chemistry, University at Albany, State University of New York, Albany, New York; and Departments of [6]Molecular Genetics and Microbiology and [7]Neurobiology, Duke University Medical Center, Durham, North Carolina

ABSTRACT   Understanding structure/function relationships of olfactory receptors is challenging due to the lack of x-ray structural models. Here, we introduce a QM/MM model of the mouse olfactory receptor MOR244-3, responsive to organosulfur odorants such as (methylthio)methanethiol. The binding site consists of a copper ion bound to the heteroatoms of amino-acid residues H105, C109, and N202. The model is consistent with site-directed mutagenesis experiments and biochemical measurements of the receptor activation, and thus provides a valuable framework for further studies of the sense of smell at the molecular level.

Olfactory receptors (ORs) belong to the family of seven transmembrane (TM) G-protein-coupled receptors (GPCRs) that respond to exogenous chemical ligands (1,2). The signal transduction mechanism is dependent on the shape and concentration of the odorant ligand in the nasal aqueous mucus, and on the response kinetics as determined by specific odorant-OR interactions at the binding site (3,4). Studies of olfactory response at the molecular level, however, are currently hindered by the lack of molecular structures of ORs. This is partially due to the usual technical difficulties in expression and crystallization of GPCRs (5). In addition, the characterization of receptor binding sites with metal centers is particularly challenging (6). Therefore, it is imperative to combine biochemical studies (7,8) and computational modeling techniques (9,10) to develop structural models of ORs that could be tested against mutagenesis experiments and activation profiles.

This letter reports a structural model of the mouse olfactory receptor MOR244-3 (Fig. 1), responsive to organosulfur odorants, such as MTMT ((methylthio)methanethiol) found in the urine of fertile male mice (7). MOR244-3 has been recently reported to require copper for robust ligand binding and activation (11), although a structural model of the ligand binding site has yet to be established. The MOR244-3 model is built at the M06-L level of density functional theory (12) in conjunction with quantum mechanics/molecular mechanics (QM/MM) hybrid methods (13), and homology modeling (14) using the x-ray structure

of the human M2 muscarinic (M2) receptor (15) as a template. The comparative protein modeling by satisfaction of spatial restraints (14) against the available x-ray structures in the literature indicates a high sequence identity between the MOR244-3 and M2 receptor TM regions (see Fig. S1 and Fig. S2 in the Supporting Material). The QM/MM calculations are based on the two-layer ONIOM method with electronic-embedding scheme (13). Electronic embedding incorporates the point charges of the MM region into the QM Hamiltonian. This technique provides a description of the electrostatic interaction between the QM and MM regions (as it is treated at the QM level) and allows the QM wavefunction to be polarized (16). The resulting density functional theory QM/MM level ensures a more reliable description of Cu-ligand interactions than MM or MM-MD modeling.

An important structural feature exhibited by the proposed MOR244-3 model is the internal aqueous channel (Fig. 1 a, green) that extends from the extracellular surface through the ligand binding pocket into a depth of ~30 Å, where it is interrupted by a hydrophobic cap (Fig. 1 a, blue) formed by L66 and L114. These two residues also form an analogous hydrophobic cap that separates the extracellular and
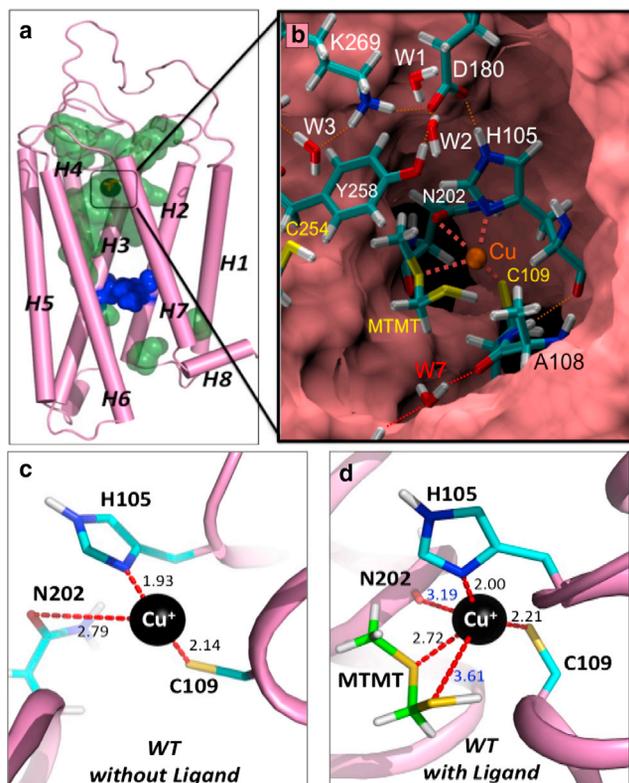

CrossMark

FIGURE 1 (*Top*) (*a*) QM/MM model of the MOR244-3, including an aqueous channel (*green*) inside the barrel of TM α-helices (*pink*). (*b*) MTMT bound to Cu$^+$ coordinated to the heteroatoms of H105 and C109, and surrounded by a cage of H-bonds linking H105, D180, K269, Y258, and water molecules. (*Bottom*) The active site of MOR244-3 without (*c*) and with (*d*) the MTMT ligand.

described below, however, C109 is more consistent with mutagenesis studies. In contrast, C179 is a conserved amino-acid residue essential for disulfide bond formation with C97. The disulfide bond links the EII loop and the TM3 regions and is conserved in other ORs, including MOR256-17, which responds to MTMT but does not exhibit a Cu enhancement effect on activity (11). Conserved amino-acid residues and structural motifs were found through the alignment of MOR244-3 and MOR256-17 primary sequences (Fig. 2 *a*). The alignment was also useful to explore several other possible binding sites for Cu, where pairs of His/Cys amino-acid residues are sufficiently close (within 3.0 Å of each other) to coordinate to a common metal center, including C240/H243, C72/H73, C127/H131, and H155/C210, in addition to H105/C109 (Fig. 2 *a*). However, the C240/H243 pair was found unlikely to be the active site because it is conserved in both MOR244-3 and MOR256-17, and MOR256-17 is insensitive to Cu. Of the other three, C72/H73 and H155/C210 pairs were ruled out because activity was unchanged by the mutations C72V, H73Y, H73F, C210S, and C210A (11). In addition, the mutation H155R prevented the expression of the receptor at the surface altogether, leaving the H105/C109 pair as the only site supported by mutagenesis analysis (11).

The proposed coordination of Cu$^+$ to H105 and C109 is consistent with mutagenesis analysis. H105 mutants yield a loss-of-function phenotype in receptor functional assays (11). In addition, the C109V mutant model (Fig. 3 *a*) shows that the substitution of cysteine by valine replaces the thiolate (–S$^-$) by the larger isopropyl group -CH(CH$_3$)$_2$, leading

cytoplasmic parts of the water channel in the homology M2 receptor (15). The ligand-binding site (Fig. 1 *b*) consists of Cu$^+$ coordinated to the heteroatoms N, S, and O of amino-acid residues H105, C109 (in thiolate form), and N202, respectively, in the aqueous channel. In the absence of a ligand, Cu$^+$ adopts a linear coordination with N$_{H105}$ and S$_{C109}$ and a weak interaction with O$_{N202}$ (Fig. 1 *c*). Upon MTMT binding, the SMe$_{MTMT}$ group exchanges with the O$_{N202}$ ligand and induces Cu$^+$ to adopt a trigonal planar coordination with N$_{H105}$, S$_{C109}$, and SMe$_{MTMT}$ (Fig. 1 *d*). A cage of H-bonds linking the amino-acid residues H105, D180, K269, Y258, T259, F256, I255, C254, and S207, and water molecules encloses the binding site and forms a lid over the organosulfur ligand (Fig. 1 *b*). Some of these structural features are similar to those found in the active sites of other heptahelical TM proteins (17), and the coordination of Cu to the heteroatoms of histidine and cysteine residues in other metalloproteins (e.g., azurin). The coordination of Cu is also consistent with previous studies that suggested the coordination to a soft anionic center (e.g., RS$^-$) because Cu has high affinity for thiols (6).

Other cysteine residues, such as C179, have been proposed as potential candidates for Cu binding (18). As
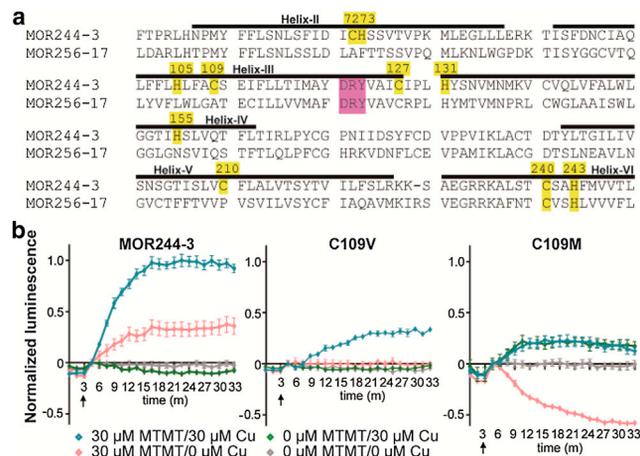

FIGURE 2 (*a*) Partial primary sequence alignment between MOR244-3 and MOR256-17. (*Yellow*) Cysteine/histidine (i.e., C, H) pairs within 3.0 Å of each other in the homology models. (*Black lines*) Helices II–VI. (*Magenta*) Conserved DRY motif. (*b*) Real-time measurement of activity of MOR244-3 WT, C109V, and C109M mutants in the presence of 30 μM Cu^{2+} and/or 30 μM MTMT, using the GloSensor (Promega) assay. (*Arrows*) Timepoint of odorant addition. The *y* axis represents mean luminescence mean $\pm$ SE, normalized to the response of wild-type MOR244-3 to 30 μM Cu^{2+} and 30 μM MTMT (*N* = 6).
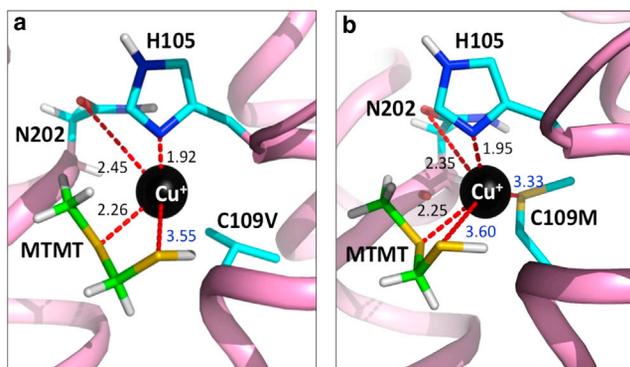
FIGURE 3   QM/MM optimized models of the MOR244-3 C109V (*a*) and C109M (*b*) mutants with MTMT bound to Cu$^+$. Coordination distances (*dashed lines*) are in Ångstroms.

to the loss of coordination of Cu$^+$ to site 109 even when MTMT binds to H105. As a result, the C109V mutant deprives Cu$^+$ of one of its key ligands and exhibits reduced functionality (Fig. 2 *b*). Activity diagrams of mutants C72V, H73Y, H73F, C210S, and C210A are available in Fig. S3 of Duan et al. (11).

The GloSensor assay (Promega, Madison, WI) also shows that the C109M mutant is activated in the presence of Cu, while MTMT exerts an inverse agonist effect on the receptor activation (Fig. 2 *b*). Consistently, the C109M mutant model (Fig. 3 *b*) shows that the coordination sphere of Cu$^+$ replaces the negatively charged thiolate (–S$^-$) group by a thioether (–SCH$_3$) ligand. This change reduces the distances Cu—SMe$_{MTMT}$ and Cu—O$_{N202}$ (Fig. 3 *b*), while increasing the distance Cu—S$_{C109M}$ (Fig. 3 *b*). These results are consistent with an inverse agonist effect due to competitive binding of SMe$_{MTMT}$ and S$_{C109M}$ to Cu$^+$. Furthermore, we find that chelators of Cu$^+$, such as TEPA (tetraethylenepentamine), antagonize the activation of the C109M mutant, likely due to the removal of Cu from the system (see Fig. S3).

In addition to the analysis of mutants, we find that the calculated relative stability of various organosulfur ligands correlates well with the observed changes in the receptor response, as monitored by GloSensor assays (Promega). For example, we find that the binding energy of MTMT is −23.4 kcal/mol, relative to MTMT in aqueous solution (see Table S1, Table S2, Table S3, Table S4, and Fig. S4 in the Supporting Material). In contrast, methanedithiol (HSCH$_2$SH) is predicted to have less affinity to bind to the MOR244-3 binding pocket (by 0.6 kcal/mol) compared to MTMT, because it does not coordinate with the Cu$^+$ ion (see Table S1, Table S4, and Fig. S5). These data correlate well with the significant response of MOR244-3 toward MTMT and to the lack of response toward HSCH$_2$SH (see Fig. S6). We note that the main difference between the two ligands is the presence of the thioether group in MTMT, which seems to be critical for ligand binding to Cu$^+$ in MOR244-3. Consistently, other organosulfur

ligands that lack the thioether group (e.g., CH$_3$SSCH$_3$, HS(CH$_2$)$_2$SH) exhibit no activity, whereas ligands with thioether groups (e.g., CH$_3$S(CH$_2$)$_2$SH, CH$_3$CH$_2$SCH$_2$SH) show high response (see Fig. S7) (11).

In summary, our combined experimental and computational analysis supports an atomistic structural model of the MOR244-3 binding site that consists of Cu bound to H105, C109, and N202 in an internal aqueous channel of the TM GPCR. The model is consistent with mutagenesis studies and biochemical measurements of the receptor activation, as induced by various organosulfur odorants with thioether groups. The reported QM/MM model should be particularly valuable for studies of mammalian olfaction at the molecular level.

SUPPORTING MATERIAL

Experimental Details, Computational Details, seven figures, and four tables are available at http://www.biophysj.org/biophysj/supplemental/S0006-3495(14)00750-4.

ACKNOWLEDGEMENTS

REFERENCES and FOOTNOTES

1. Buck, L., and R. Axel. 1991. A novel multigene family may encode odorant receptors: a molecular basis for odor recognition. *Cell.* 65: 175–187.

2. Firestein, S. 2001. How the olfactory system makes sense of scents. *Nature.* 413:211–218.

3. Breer, H., I. Boekhoff, and E. Tareilus. 1990. Rapid kinetics of second messenger formation in olfactory transduction. *Nature.* 345: 65–68.

4. Touhara, K., and L. B. Vosshall. 2009. Sensing odorants and pheromones with chemosensory receptors. *Annu. Rev. Physiol.* 71: 307–332.

5. Kaiser, L., J. Graveland-Bikker, …, S. Zhang. 2008. Efficient cell-free production of olfactory receptors: detergent optimization, structure, and ligand binding analyses. *Proc. Natl. Acad. Sci. USA.* 105:15726–15731.

6. Crabtree, R. H. 1978. Copper (I): a possible olfactory binding site. *J. Inorg. Nucl. Chem.* 40:1453.

7. Lin, D. Y., S. Z. Zhang, …, L. C. Katz. 2005. Encoding social signals in the mouse main olfactory bulb. *Nature.* 434:470–477.

8. Kato, A., S. Katada, and K. Touhara. 2008. Amino acids involved in conformational dynamics and G protein coupling of an odorant receptor: targeting gain-of-function mutation. *J. Neurochem.* 107:1261–1270.

9. Kurland, M. D., M. B. Newcomer, …, V. S. Batista. 2010. Discrimination of saturated aldehydes by the rat I7 olfactory receptor. *Biochemistry.* 49:6302–6304.

10. Gelis, L., S. Wolf, …, K. Gerwert. 2012. Prediction of a ligand-binding niche within a human olfactory receptor by combining site-directed mutagenesis with dynamic homology modeling. *Angew. Chem. Int. Ed. Engl.* 51:1274–1278.

11. Duan, X., E. Block, …, H. Zhuang. 2012. Crucial role of copper in detection of metal-coordinating odorants. *Proc. Natl. Acad. Sci. USA.* 109:3492–3497.

12. Zhao, Y., and D. G. Truhlar. 2006. A new local density functional for main-group thermochemistry, transition metal bonding, thermochemical kinetics, and noncovalent interactions. *J. Chem. Phys.* 125:194101.

13. Vreven, T., K. Morokuma, …, M. J. Frisch. 2003. Geometry optimization with QM/MM, ONIOM, and other combined methods. I. Microiterations and constraints. *J. Comput. Chem.* 24:760–769.

14. Sali, A., and T. L. Blundell. 1993. Comparative protein modeling by satisfaction of spatial restraints. *J. Mol. Biol.* 234:779–815.

15. Haga, K., A. C. Kruse, …, T. Kobayashi. 2012. Structure of the human M2 muscarinic acetylcholine receptor bound to an antagonist. *Nature.* 482:547–551.

16. Sekharan, S., and K. Morokuma. 2011. Why 11-*cis*-retinal? Why not 7-*cis*-, 9-*cis*-, or 13-*cis*-retinal in the eye? *J. Am. Chem. Soc.* 133:19052–19055.

17. Sekharan, S., V. L. Mooney, …, V. S. Batista. 2013. Spectral tuning of ultraviolet cone pigments: an interhelical lock mechanism. *J. Am. Chem. Soc.* 135:19064–19067.

18. Wang, J., Z. A. Luthey-Schulten, and K. S. Suslick. 2003. Is the olfactory receptor a metalloprotein? *Proc. Natl. Acad. Sci. USA.* 100:3035–3039.